Homeostasis of Peripheral Immune Effectors

Christina Warrender [a,*] Stephanie Forrest [a,c] Lee Segel [b]

[a] *Department of Computer Science, 1 University of New Mexico, Albuquerque, NM 87131-0001, USA*

[b] *Department of Computer Science and Applied Mathematics, The Weizmann Institute of Science, Rehovot 76100, Israel*

[c] *Santa Fe Institute, 1399 Hyde Park Rd., Santa Fe, NM, 87501, USA*

Abstract

In this paper, we use both mathematical modeling and simulation to explore homeostasis of peripheral immune system effector cells, particularly alveolar macrophages. Our interest is in the distributed control mechanisms that allow such a population to maintain itself. We introduce a multi-purpose simulator designed to study individual cell responses to local molecular signals and their effects on population dynamics. We use the simulator to develop a model of growth factor regulation of macrophage proliferation and survival. We examine the effects of this form of regulation in the context of two competing hypotheses regarding the source of new alveolar macrophages. In one model, local cells divide to replenish the population; in the other, only cells migrating from circulation divide. We find that either scenario is plausible, although the influx-driven system is inherently more stable. The proliferation-driven system requires lower cell death and efflux rates than the influx-driven system.

1 Introduction

The number of immune system effector cells in peripheral tissues remains fairly constant in the absence of disease, despite a large amount of turnover. Populations change through proliferation, death, and migration of individual cells. These functions are regulated by various molecular mediators known as cytokines, but we are just beginning to understand how cells interpret and

* Corresponding author.

Email addresses: christy@cs.unm.edu (Christina Warrender), forrest@cs.unm.edu (Stephanie Forrest), lee.segel@weizmann.ac.il (Lee Segel).

Preprint accepted by the Bulletin of Mathematical Biology *11 March 2004*

respond to the information in the local molecular environment. The goal of this work is to investigate what kinds of cell 'programming' can cause appropriate population-level behavior. Rather than simply plugging the observed growth rates in to population models, we would like to understand how such population-level rates are related to individual cell responses to local molecular signals. What are the regulatory mechanisms that maintain an appropriate balance between individual cell actions?

The regulatory signals that allow maintenance of a steady-state population are of interest in their own right, and also have an impact on the changes to that population when foreign organisms are encountered. Maintenance of an appropriate 'sentinel' population enables rapid initiation of an immune response in case of infection, and homeostatic regulation plays a role in restoring normal tissue function once the infection has been resolved.

This paper explores simple models of peripheral effector population homeostasis, focusing on alveolar macrophages for concreteness. Alveolar macrophages provide the first line of defense against microorganisms entering through the lungs. They are more easily studied than other macrophages because they are easily retrieved from the lungs. We also assume that alveolar macrophages are—to some degree—representative of bone-marrow-derived peripheral effectors in general, in that similar regulatory mechanisms are likely to be used in many peripheral effector populations.

We first develop a model of growth factor effects on individual cell survival and proliferation. We then use this model to investigate two alternatives for population maintenance *in vivo*: one in which proliferation of resident cells replenishes the macrophage population, and the other in which cells migrating from circulation are the only cells that divide.

Evaluating the dynamics produced by these models requires a simulator designed to handle events on both the molecular and cellular scale, with a mix of deterministic and stochastic processes. We introduce such a simulator, designed to accommodate the current model and also future models describing more complex aspects of intercellular signalling.

The next section presents background information on population dynamics of alveolar macrophages. Section 3 describes the simulator design. Section 4 develops the model of macrophage interactions with growth factor, and sections 5 and 6 explore two alternative models of macrophage homeostasis. Implications of autocrine regulation are discussed in section 7. Related work is reviewed in section 8, and a general discussion appears in section 9.

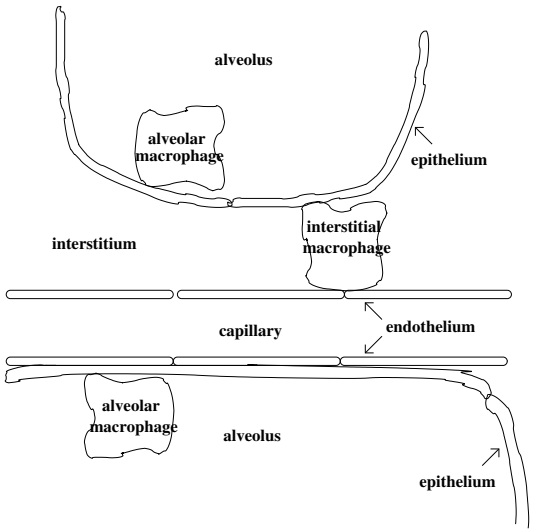

Fig. 1. Interstitial macrophages reside within pulmonary tissue; alveolar macrophages are found 'outside' the alveolar epithelium. Cells may be recruited to the alveoli from the interstitium, across the alveolar epithelium, or from circulation, across both the vascular endothelium and the alveolar epithelium.

2 Alveolar Macrophage Dynamics

Pulmonary macrophages are classified according to where they are found. Interstitial macrophages reside within lung tissue; alveolar and airway macrophages are found along the epithelium of the alveoli and branching airways, respectively. Figure 1 is a sketch of macrophages in and around alveoli. Macrophages in different locations, and even within a single location, show great morphological and functional heterogeneity (Laskin *et al.*, 2001), making the exact relationship between these various subpopulations unclear. Also, macrophages are highly mobile, capable of moving both within and between compartments. As a result, there are several factors affecting the size of local populations: differentiation, migration, proliferation, and death. All of these cell behaviors are somehow kept in balance during normal conditions, but rapidly expand the population in response to infection or injury.

The origin of alveolar macrophages has not been completely resolved. Van Furth (1992) proposed that all macrophages in peripheral tissues, including the lung, are part of a mononuclear phagocyte system (MPS). This system consists of cells that derive from bone marrow precursors, which differentiate into blood monocytes that randomly leave the circulation to enter various tissues and become macrophages. The tissue macrophages were thought to be terminally differentiated and incapable of proliferating. Others, however, have argued that local proliferation is important and may even be primarily responsible for maintaining alveolar macrophage populations (Coggle and Tarling, 1984; Shellito *et al.*, 1987). Alveolar macrophages are capable of proliferating *in vitro*

in the presence of the appropriate molecular growth factors (Lin *et al.*, 1989; Akagawa *et al.*, 1988), in contrast to expectations for terminally differentiated cells. Also, *in vivo* labelling studies have shown that roughly 3% of alveolar macrophages are synthesizing DNA in preparation for cell division at any given time (Blusse van Oud Alblas *et al.*, 1983; Coggle and Tarling, 1984; Fritsch and Masse, 1992), but the authors disagree about which cells are dividing. Several theories for the origin of alveolar macrophages have been proposed and investigated:

(1) Alveolar macrophages derive from migrating blood monocytes, and are normally incapable of dividing (Blusse van Oud Alblas and van Furth, 1979);
(2) Monocytes mature in lung capillaries and undergo a final maturation division in the alveoli (Fritsch and Masse, 1992);
(3) Alveolar macrophages derive from interstitial macrophages through local division and maturation (Bowden, 1984);
(4) Alveolar macrophages divide *in situ* (Coggle and Tarling, 1984; Shellito *et al.*, 1987).

There are also multiple ways in which macrophages may leave the alveoli. The most common route out of the alveoli is up the bronchi to where they can be expelled or swallowed (Perez-Arellano *et al.*, 1990). Trafficking of alveolar macrophages to the lymph nodes has also been reported (Corry *et al.*, 1984; Harmsen *et al.*, 1985), and some other routes have a minor role (Perez-Arellano *et al.*, 1990). Cell death is also a significant factor. It is often difficult to determine whether cell loss is due to migration or death; quantitative studies often measure a simple loss rate that does not distinguish between the various migration routes and cell death (Fritsch and Masse, 1992).

The studies referenced above attempted to quantify the rates of local proliferation, influx, death, and/or efflux, but did not address the mechanisms involved. Each of these activities depends on interactions between macrophages and the appropriate molecular signals in the environment or on other cells. In this paper, we focus on the effects of macrophage colony stimulating factor (M-CSF) on macrophage proliferation and survival.

There are a number of molecular mechanisms that regulate a cell's transition from the resting state to the proliferating state and its progression through the cell cycle. In particular, the proper growth factor(s) must be present before a cell can pass a restriction point and begin DNA synthesis (Pardee, 1989) The time required between the beginning of DNA synthesis and cell division is fairly constant, but the time between one division and beginning of DNA synthesis for the next is highly variable. Increasing concentrations of growth factor can shorten this time and therefore the total cell cycle time (Metcalf, 1991). Pardee (1989) proposed that growth factor binding drives accumulation

of a rapidly decaying internal substance which must reach a critical level for the cell to begin synthesizing DNA, and Smith (1989) found that a critical number of such bindings must be reached for T cells to divide.

Macrophage-Colony Stimulating Factor (M-CSF) and Granulocyte-Macrophage-Colony Stimulating Factor (GM-CSF) have both been shown to stimulate division of murine alveolar macrophages *in vitro* in a dose-dependent fashion (Chen *et al.*, 1988; Akagawa *et al.*, 1988; Lin *et al.*, 1989). Injection of M-CSF has also been shown to increase alveolar macrophage numbers *in vivo* (Held *et al.*, 1996).

In addition to promoting cell proliferation, growth factors are believed to promote cell survival by preventing apoptosis (Williams *et al.*, 1990), although dose dependence has not been studied as extensively as it has been for proliferation. Tushinski *et al.* (1982) showed that macrophages cultured without M-CSF died, and that a low dose could maintain macrophage populations *in vitro* with little proliferation.

3 The CyCells Simulator

In order to study the cellular responses to molecular signals described above, we have developed a discrete-time simulator, CyCells, in which individual cells are represented explicitly and molecules are represented by their concentration. The behavior of different types of cells and molecules is specified at run time, as described below. There is significant flexibility in the way cell types can be defined, and a number of different cell and molecule types can be combined in any given model. CyCells was written in C++ and is publicly available at `http://www.cs.unm.edu/~christy/simcode`.

3.1 Model Definition

A model definition file like the one shown in Figure 2 specifies the behavior of each molecule and cell type used in a simulation. The file consists of a list of cell type names, followed by a block for each molecule type and a block for each cell type.

Molecule types are defined by giving them a name and specifying the appropriate decay and/or diffusion rates. Note that cells can also change the molecular concentration by secreting or binding molecules. Although there is only one molecule type in the example, multiple molecule types are allowed.

A cell type definition specifies the attributes all cells of that type have, how

```
cell_names { macrophage cycling tissue }

molecule_type CSF {
decay_rate 1e-4
}

cell_type macrophage {
attribute cmax lognormal 3.58 0.4 lognormal 3.58 0.4
attribute b fixed 0 fixed 0
attribute S fixed 0 uniform 0 700000
attribute sr gaussian 700000 50000 gaussian 700000 50000
attribute time fixed 0 fixed 0
attribute tc gaussian 43200 1800 gaussian 43200 1800
sense b consume-indiv CSF cmax 1.3E-13
process S update linear b 1 0
action change cycling gte_var S sr
action die calc_prob inhibiting b 1e-5 0.37
}

cell_type cycling {
attribute cmax lognormal 3.58 0.4 lognormal 3.58 0.4
attribute b fixed 0 fixed 0
attribute S fixed 0 uniform 0 700000
attribute sr gaussian 700000 50000 gaussian 700000 50000
attribute time fixed 0 uniform 0 43200
attribute tc gaussian 43200 1800 gaussian 43200 1800
sense b consume-indiv CSF cmax 1.3E-13
process time update fixed 1
action divide macrophage gte_var age tc
}

cell_type tissue {
action secrete CSF fixed 2 always
}
```

Fig. 2. Sample model definition file.

```
geometry
1000x1000x1000 microns; mol_res:  0  cell_res:  0

molecule_uniform:  CSF 6E-15 0

cell_count:  tissue 1000
cell_count:  cycling 30
cell_count:  macrophage 970
```

Fig. 3. Sample model initialization file.

those attributes should be initialized, and how they should be updated or used to make decisions during each time step. The actual values of those attributes are stored for each individual cell. In the example shown in Figure 2, macrophages have six attributes. Some of these are initialized at specific values, while others are chosen from uniform, gaussian, or lognormal distributions. There are two initialization specifications because cells may be initialized either as new daughter cells or as cells entering the simulation in the middle of the life cycle; the macrophage attribute S is initialized differently for these two different situations.

The simulator treats sensing, intracellular signalling and actions as different kinds of cell functions that use or update cell attributes. Cells may die, divide, differentiate, migrate, or secrete molecules. Some of these actions are

constitutive, others depend on cell state. For the latter, intracellular processing functions determine how a cell's current state and its perception of the local environment are combined to update the cell state. They are an abstraction of the complex signalling that goes on inside real cells. Sensing functions update cell variables in accordance with the current molecular concentration and may remove molecules from the environment in the process (as explained in section 4.1).

The model definition includes a line for each such function used by each cell type, with the relevant parameter values. The example shown in Figure 2 corresponds to the model described in section 4. The cell definitions used in this simulation are quite simple; more functions of each type may be added for more complex models.

3.2 Model Initialization

An initialization file, like the one shown in Figure 3, specifies the simulation geometry, initial molecular concentration(s), and initial numbers of each cell type. The simulation works with a three-dimensional volume which may divided into regular cubes, or grids, where the grid size determines the spatial resolution. However, it is also possible to treat the entire volume as one cube, in which case the simulation represents a homogeneous molecular environment. We use the latter approach in the current simulations. Cell positions can be specified if desired; in this example, cells are positioned randomly.

3.3 Simulation Execution and Order Effects

One time step of the simulation consists of the following sequence of activities:

(1) Molecular diffusion and decay
(2) Update of each cell according to sense, process, and act functions
(3) Cell movement (if applicable)

In real biological systems, molecular interactions, cellular actions and interactions between cells and molecules all happen in parallel. Imposing an order on these activities for computer execution can introduce artifacts that do not represent behaviors seen in the real system. In step (2), each cell may modify the molecular environment and thus indirectly affect cells visited later. To minimize cumulative effects of this serialization of an inherently parallel process, the cell visitation order is randomized each time step.

Order effects can also be reduced by using small time steps. However, execution time is inversely proportional to time step size, so there are practical limits on how small a time step can really be. The choice of an appropriate time step must also reflect the characteristic rates of the modeled system. The time step size is chosen by the user at run time. For the simulations in this paper, the time step was set to 10 seconds.

Simulation run time is directly proportional to the number of time steps T. For each time step, the molecular concentrations are updated in a time that is proportional to the number of grids M, and cells are updated in a time that is proportional to the number of cells N. The exact time for the cell updates will depend on the number of sensing, processing, and action functions required for each cell. Overall run time is of the form $T(aM + bN)$, where a represents the time it takes to update each grid, and b represents the average time to update each cell. Note that the number of cells is not constant, but for the simulations presented here, it does not vary significantly.

4 Macrophage Proliferation and Survival Model

This section develops our model of macrophage proliferation and survival. We rely on literature describing macrophage dependence on macrophage colony stimulating factor (M-CSF), first reviewing how macrophages sense M-CSF, and then the cellular response to sensed M-CSF.

4.1 Receptor-Ligand Binding

Molecular mediators such as growth factors affect cells by binding to cell surface receptors. Free receptors on the cell surface bind to extracellular ligand to form receptor-ligand complexes. Using R_s for free receptors (#/cell), C_s for bound complexes (#/cell), and L for ligand concentration (moles/liter), the following equations describe this process (Lauffenburger and Linderman, 1993):

$$\frac{dR_s}{dt} = -k_f L R_s + k_r C_s - k_{eR} R_s + V_s \tag{1}$$

$$\frac{dC_s}{dt} = k_f L R_s - k_r C_s - k_{eC} C_s \tag{2}$$

where k_f and k_r are the association and dissociation rate constants. Free and bound receptors may be internalized at rates k_{eR} and k_{eC}, respectively. New receptors are synthesized at rate V_s. Intracellular signal transduction is initiated when receptors become bound on the cell surface. We do not model these

effects in any detail; instead we assume that the signal affecting cell behavior is proportional to $k_f L R_s$.

In the presence of slowly varying ligand concentration, the system comes to a quasi-steady state ($dC_s/dt \approx 0$, $dR_s/dt \approx 0$) in which the numbers of cell-surface receptors and cell-surface complexes depend on L as follows (Lauffenburger and Linderman, 1993):

$$R_s = \frac{(k_r + k_{eC})C_s}{k_f L} \tag{3}$$

$$C_s = \frac{K_{ss} V_s L}{k_{eC}(1 + K_{ss} L)} \tag{4}$$

K_{ss} is a dimensionless parameter known as the apparent cellular affinity constant.

The change in ligand concentration is given by:

$$\frac{dL}{dt} = (-k_f L R_s + k_r C_s)n \tag{5}$$

where n is the cell density. The rate at which a single cell 'consumes' ligand is

$$c(L) = k_{eC} C_s = \frac{V_s K_{ss} L}{1 + K_{ss} L} = \frac{V_s L}{1/K_{ss} + L} \tag{6}$$

For growth factors, a significant amount of internalization of bound receptors always occurs (Lanza *et al.*, 2000). M-CSF in particular is rapidly internalized and degraded by macrophages (Chen *et al.*, 1984; Guilbert and Stanley, 1986). In this case, ligand binding by cells may have a significant effect on the local concentration. It also means that the rate at which ligand is internalized is roughly equal to the rate of cell signalling, since the second term of equation (5) is negligible.

Equation (6) has the general saturating form

$$c(L) = \frac{c_{max} L}{c_{half} + L} \tag{7}$$

in which c_{max} represents the maximum rate at which a cell can bind and internalize ligand (in molecules/cell sec), and c_{half} represents the ligand concentration at which the consumption rate is half of the maximum. Tushinski *et al.* (1982) measured the rate at which macrophages remove extracellular ligand at various different concentrations, which gives us estimates of c_{max} and c_{half}.

This description represents binding in the average case. However, macrophages demonstrate significant heterogeneity in the numbers of surface molecules they

express (Laskin *et al.*, 2001). As demonstrated above, the rate at which cells consume growth factor is directly proportional to the receptor synthesis rate, so variation in receptor expression should be directly correlated with variation in the maximum consumption rate c_{max}. We represent cell heterogeneity by giving each cell a different value of c_{max}, using a log-normal distribution as was used in Burke *et al.* (1997) for T cells.

4.2 Proliferative Response

Following other modelers (Zandstra *et al.*, 2000; Burke *et al.*, 1997) and evidence in the experimental literature (Chen *et al.*, 1987; Smith, 1989), our model assumes that some threshold amount of bound growth factor is required for a cell to pass the restriction point. Equation (7) represents the rate at which growth factor is bound. Each simulated cell has an internal variable S which tracks the cumulative signal received. If S reaches a positive threshold value s_r, the cell passes the restriction point and divides a fixed amount of time t_c later.

S does not represent any real molecular species inside cells; it is instead an abstract measure of the progress a cell has made towards the restriction point. In real cells, progress towards the restriction point is the result of competition between production and degradation of intracellular molecules that regulate the cell cycle. We are assuming that the net result of these competing processes is proportional to the number of receptor-ligand binding events. Because Tushinski *et al.* (1982) report some proliferation even at low growth factor concentrations, we assume that this net effect is always nonnegative. This model does not account for cell behavior in the complete absence of growth factor; cells become quiescent when growth factor is removed, and require a lag period of several hours after re-introduction of growth factor to reenter the cell cycle (Tushinski and Stanley, 1985). This would require a decrease in S during the starvation period. However, it's not clear that this implies the need for decay in S in the presence of growth factor. For simplicity, and because all of our simulations use nonzero growth factor concentrations, we omit a mechanism for decreasing S.

To summarize:

$$\Delta S = c(L)\Delta t \tag{8}$$

$$S > s_r : \text{cell will divide after time } t_c \tag{9}$$

In the absence of growth factor, macrophage populations *in vitro* exhibit exponential decay (Tushinski *et al.*, 1982) at a rate d_{max}. However, the rate at which the population decays decreases as the growth factor concentration is increased. We assume that resting cells have some probability of dying that depends on the current growth factor concentration, or more properly, on the cell's perception of the growth factor concentration. Based on an analysis of the data in Tushinski *et al.* (1982), we choose the following form for a cell's probability of dying in a small time δt:

$$p(d) = \frac{d_{max} d_{half}}{c(L) + d_{half}} \delta t \tag{10}$$

which drops off rapidly at first and then gradually approaches 0; the probability is half its maximal value when $c(L) = d_{half}$. We assume that the death rate for cells past the restriction point is negligible.

At the population level, the internalization and destruction of growth factor by macrophages could be important, as it indicates that regulation of cell populations might be at least partly controlled by competition for growth factor. Consumption of ligand completes a negative feedback loop in which increasing numbers of cells decrease the ligand concentration, which then causes a reduction in cell numbers.

4.4 Model Summary and Validation

We used CyCells with the model described above to reproduce the results reported in table 1 of Tushinski *et al.* (1982). In this experiment, 300,000 bone-marrow-derived macrophages were kept in culture with varying amounts of M-CSF for three days, with the culture medium replaced each day. At the end of that time Tushinski *et al.* measured the total cell population and percentage of cells in S phase. The cells had been cultured for several days in M-CSF before the beginning of the experiment; a control experiment showed that one-third of the initial cell population was in S phase at the beginning of the experiment.

To simulate this experiment, we define two cell types to represent resting and cycling cells. This is a modeling convenience; both 'types' represent macrophages, and individual cells may change type during the simulation. All cells consume growth factor as described in section 4.1. Resting cells use the amount of growth factor bound to increment their internal S value as described in section 4.2. Cells with an S value greater than or equal to s_r becoming cycling

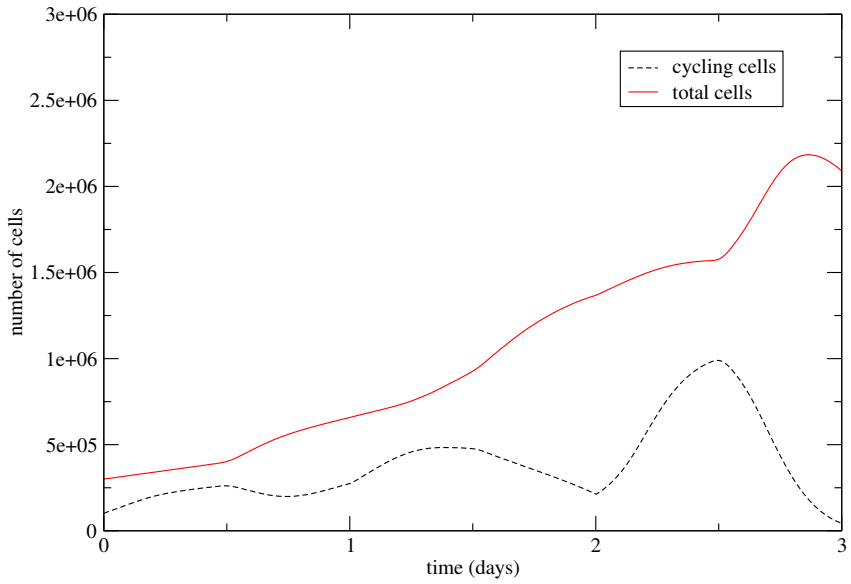

Fig. 4. Total cell population and number of cycling cells for simulation of Tushinski's experiment at high growth factor concentration (set to 4.4×10^{-10} M at the start of each day). Parameter values shown in table 1.

cells. These cells track how long they have been in the cell cycle, and divide—producing two resting cells—after time t_c. Resting cells die with a probability calculated as in section 4.3; dividing cells do not.

We initialized the simulations with 100,000 cycling cells and 200,000 resting cells. Different simulations used different initial growth factor concentrations, in accordance with (Tushinski *et al.*, 1982), and the growth factor concentration was reset to the initial value at the beginning of each simulated day. We found reasonable agreement with the final population sizes in (Tushinski *et al.*, 1982) using the parameter values shown in table 1. These values are used in the following sections. Small variations in t_c and s_r also give reasonable results; variations in these parameters are much less significant than variations in the death rate.

However, the simulations show significant variation in the percentage of cycling cells, as shown in figure 4. Tushinski *et al.* (1982) naturally report only the initial and final percentages of S-phase cells. In simulation, we have the opportunity to observe more detailed dynamics than can be observed in culture experiments. First, since roughly a third of the cell population is already committed to divide at the start of the experiment, there is always an initial increase in the cell population regardless of ligand concentration. This initial burst is amplified in the runs with higher ligand concentration as more cells enter the cell cycle, and is followed by a period when large numbers of cells divide and few are left in the cell cycle. Second, there is significant ligand depletion for most of the experiments in between the daily replenishments. Since Tushinski *et al.* (1982) measured M-CSF removal, this is not really surprising,

	Meaning	Mean value
c_{max}	maximum consumption rate	36 molecules/sec
c_{half}	concentration for half-maximal consumption	1.3×10^{-10} M
s_r	restriction point threshold	700,000
t_c	cell cycle time	12 hours
d_{max}	maximum death rate	1×10^{-5} /sec
d_{half}	consumption rate for half-maximal death	.37 molecules/sec

Table 1
Parameters affecting macrophage proliferation and survival. Note that individual cells each have different values of c_{max}, s_r and t_c; the value shown is the population mean.

but we found that it causes a temporary decline in cell counts at the end of each day in otherwise-growing cell populations. These two effects produce oscillations in the ratio of cycling to resting cells. It would be interesting to see whether this kind of oscillation could be seen in culture if measurements were made more frequently.

5 Proliferation-Driven Homeostasis

We take the model developed in the previous section as a plausible model of macrophage proliferation and survival in response to M-CSF and now turn to the consequences for macrophage homeostasis *in vivo*. In this section, the population is replenished exclusively through local proliferation; in the next section, we will add influx of monocytes from the bloodstream.

5.1 Differential Equation Model

Before presenting the individual-based model and simulation results, it is helpful to start with a mathematical description of the population as a whole. We have two subpopulations of macrophages: resting cells, represented by their concentration A, and those that have passed the restriction point, represented by their concentration B. They change according to:

$$\frac{dA}{dt} = 2rB - k(L)A - l(L)A \tag{11}$$

$$\frac{dB}{dt} = -rB + k(L)A \tag{12}$$

where r is the fixed rate at which proliferating cells divide, k is the rate at which resting cells pass the restriction point, and l is the loss rate. In addition to the variable death rate used in the last section, the loss term includes efflux.

We assume that there is some source p of ligand (where p is in molecules/sec). In addition to removal by macrophages, we allow for other mechanisms of growth factor decrease with a net rate of n. M-CSF is particularly resistant to degradation by proteases (Stanley and Metcalf, 1971), but molecules can be lost to the surrounding environment. The change in ligand concentration is

$$\frac{dL}{dt} = \frac{p}{VN_{Av}} - \frac{c(L)}{N_{Av}}(A+B) - nL \tag{13}$$

(N_{Av} is Avogadro's number.) Note that although cells that have passed the restriction point no longer require growth factor, we assume that they would continue to bind and internalize growth factor.

From equations (11) and (12), we note that a steady-state system requires $k = l$. Since both of these depend on L, this determines the steady-state ligand concentration. Then, from (13), the steady-state cell density is determined by the fact that growth factor production must balance consumption and loss. In other words, the cell proliferation and survival parameters alone determine the steady-state ligand concentration, and then the growth factor production and loss rates determine the population that can be supported.

We also note that in order to have a certain fraction f of the cells dividing at any given time, as observed *in vivo*, there is another constraint on k. With $B = f(A+B)$, equation (12) implies $k = rf/(1-f)$. Because of the steady-state requirement just mentioned, the loss rate l would need to have the same value. Since $r \sim 1/t_c$, we estimate k and l to be on the order of 2%/day in order to have approximately 3% of the cells in S phase.

However, for the individual-based model, we do not choose k; although the loss rate l has a direct relation to individual cells' probabilities of dying and migrating out of the compartment, k is somewhat more complicated. The probability that an individual cell will pass the restriction point depends on its rate of binding growth factor ($c(L)$ from section 4) and on the threshold point s_r. It also depends on the loss rate, because cells must survive long enough to reach the restriction point. Some of these parameters in turn depend on the growth factor concentration, which may vary over the lifetime of the cell. Finally, there is no straightforward way to relate this individual cell probability to the instantaneous population rate k.

To implement this model in CyCells, we start with the model used in section 4 but add constitutive production of growth factor, growth factor decay, and probability of macrophage loss due to efflux. For the moment we assume that growth factor is produced by a different cell type; we will address autocrine regulation in section 7. Our simulated compartment represents a volume of 0.001 ml, which should hold approximately 1000 macrophages at normal lung densities based on estimates in (Fisher *et al.*, 1988).

Estimates for loss rates of alveolar macrophages vary widely. Fritsch and Masse (1992) reported death rates of 5–6%/day and efflux rates of 2–3%/day in rats. Other researchers do not distinguish between death and efflux, but report loss rates ranging from 1 to 18%/day (Blusse van Oud Alblas *et al.*, 1983; Coggle and Tarling, 1984; Shellito *et al.*, 1987) We ran simulations with efflux rates of 0, 5, and 10 %/day.

We first initialized the ligand concentration to 2×10^{-11} M, approximately the concentration at which cell counts changed least in Tushinski *et al.* (1982). Since we have no good estimates for growth factor production or loss rates, we chose these parameters to suit our purposes. We arbitrarily chose a growth factor loss rate of 0.006/min, and then estimated the production rate which should maintain the cell population at the chosen concentration. As mentioned earlier, the primary effect of these two parameters is on the steady-state cell density.

This simulation experiment was not entirely successful, as shown in Figure 5 for the no-efflux case. Table 2 shows the final ligand concentrations and cell numbers for all simulations. Although the system does reach a steady state, cell densities are much higher and ligand concentrations much lower than expected. By contrast, although the cell density did not change significantly for the same concentration in Tushinski's experiments, our simulation of the same experiment showed that the system was not really at steady state. Also, because ligand depletion effects were significant, the average ligand concentration actually would have been lower than 2×10^{-11} M.

Because of the feedback between growth factor concentration and cell population, the system settles at a ligand concentration at which entry into the cell cycle balances cell loss. When we choose a growth factor production rate more appropriate for this concentration, we can bring the number of cells closer to the desired value of 1000, as shown in table 3. Note that the steady-state ligand concentrations corresponding to different efflux rates are the same as seen in table 2; changing the growth factor production rate does not affect the steady-state concentration, as expected. We started these simulations with

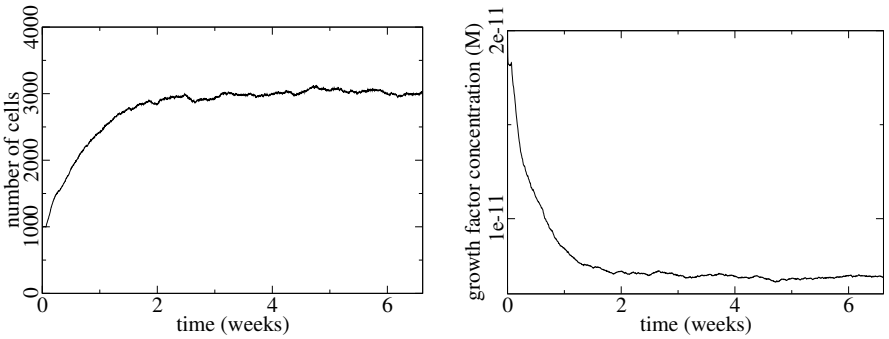

Fig. 5. Cell population (left) and ligand concentration (right) for initial simulation of proliferation-dependent homeostasis. Growth factor loss rate n: 0.006/min; production rate p: 6000 molecules/sec; no efflux. All other parameters as shown in table 1.

Efflux rate	Concentration	# cells	% cycling cells
0%/day	6.9×10^{-12} (1.1×10^{-13})	3022 (38)	7.2% (0.4%)
5%/day	8.3×10^{-12} (1.4×10^{-13})	2489 (25)	8.6% (0.5%)
10%/day	1.0×10^{-11} (9.6×10^{-14})	2021 (16)	10% (0.4%)

Table 2
Steady-state concentration and cell values for initial proliferation-driven homeostasis simulations, given as simulation mean (standard deviation). Growth factor loss rate n: 0.006/min; production rate p: 6000 molecules/sec; all other parameters as in table 1.

Efflux rate	Concentration	# cells	% cycling cells
0%/day	6.9×10^{-12} (1.5×10^{-13})	857 (20)	7.6% (0.9%)
5%/day	8.3×10^{-12} (2.3×10^{-13})	683 (20)	8.9% (1.0%)
10%/day	1.0×10^{-11} (2.7×10^{-13})	527 (16)	10% (1.5%)

Table 3
Steady-state concentration and cell values for proliferation-driven homeostasis simulations, given as simulation mean (standard deviation). Growth factor loss rate n: 0.006/min; production rate p: 2000 molecules/sec; all other parameters as in table 1.

1000 cells; it still took several days to reach the steady-state shown in table 3.

The fraction of the cell population that is dividing is about twice that observed *in vivo*. Lowering this fraction would require changing the steady-state point of the system by changing model parameters affecting cell survival and proliferation. As noted above, the loss rate would also have to be very low; the total loss rates in these runs are about 15–20%/day. A lower ligand concentration would decrease the rate at which cells commit, but would also drastically raise the death rate, so the system cannot stabilize at such a concentration.

There are a number of possible reasons for the discrepancy. It is possible that a better model of cell death would account for both the culture data and the data from alveolar macrophages *in vivo*. On the other hand, there may be significant differences between bone-marrow-derived macrophages and alveolar macrophages that the model does not address at all. Also, we take into account the effects of only a single growth factor on the macrophage population; it is likely that other mechanisms would lower the loss rate and the fraction of cycling cells *in vivo*.

6 Influx-Driven Homeostasis

We now look at a system driven primarily by influx of cells from circulation. There is still local division in this system, as observed *in vivo*, but only newly arrived cells divide.

6.1 Differential Equation Model

In this version, we still have resting and dividing macrophages (A and B, respectively), but we add monocytes (C) entering from the circulation at rate i. When the monocytes pass the restriction point, they become dividing cells, which produce resting effectors when they divide:

$$\frac{dA}{dt} = 2rB - l(L)A \tag{14}$$

$$\frac{dB}{dt} = k(L)C - rB \tag{15}$$

$$\frac{dC}{dt} = i - k(L)C - l(L)C \tag{16}$$

Note that, unlike the other terms, the influx rate does not depend on the local cell population. The number of cells migrating into the alveoli depends on the circulating precursor population; we assume here that this population is large enough to ignore possible effects of depletion. Migration of cells across the epithelial barrier into the alveolar compartment is a complex process *in vivo*, but also a relatively quick one. While division can take on the order of hours, migration generally occurs within a few minutes. We assume that influx is a random process occurring at a fixed rate.

All three cell types consume ligand:

$$\frac{dL}{dt} = \frac{p}{VN_{Av}} - \frac{c(L)}{N_{Av}}(A + B + C) - nL \tag{17}$$

Efflux rate	Concentration	# cells	% cycling cells
0%/day	5.5×10^{-12} (1.2×10^{-13})	986 (26)	2.4% (0.4%)
5%/day	6.5×10^{-12} (1.3×10^{-13})	838 (26)	2.7% (0.4%)
10%/day	7.6×10^{-12} (2.1×10^{-13})	706 (20)	3.1% (0.7%)

Table 4
Steady-state concentration and cell values for influx-driven homeostasis simulations, given as simulation mean (standard deviation). Growth factor loss rate n: 0.006/min; production rate p: 2000 molecules/sec; influx rate: 1.4 cells/ml/second; all other parameters as in table 1.

In this system, there is always a steady state, although the parameters will determine whether it is biologically feasible. In particular, we note that k and l are no longer required to be equal.

6.2 Simulations

The simulation model includes one cell type for each of the equations above. The only new parameter value is the influx rate i; we use a value of 1.4 cells/ml/second, based on estimates of monocyte migration into the lungs (Blusse van Oud Alblas *et al.*, 1983).

Results are shown in table 4. In these runs, the percentage of cycling cells is closer to that observed *in vivo*. One reason for this may be that the continual influx of new cells reduces the need for local proliferation to balance loss.

The steady-state ligand concentrations are fairly low, leading to higher death rates; even without efflux, the loss rate is around 18%/day. Death rates were unusually high in the proliferation-driven model as well, which may be an artifact of our macrophage model. However, comparing the two homeostasis models still shows higher loss rates in the influx model than the proliferation model. It seems reasonable that a constant influx of new cells would be balanced by higher loss rates; this system has greater cell turnover. This increased turnover also allows the system to recover from perturbation more quickly than the proliferation-driven model (data not shown).

7 Autocrine Regulation

Equations (13) and (17) assumed constant-rate production of ligand by some source other than the effectors, representing a strictly paracrine control system. But mature macrophages are capable of producing M-CSF (Becker *et al.*,

1989). To explore the possible effects of autocrine regulation, we ran some simulations in which all of the cells produce their own growth factor. The secretion rate was chosen so that a population of 1000 cells would produce the same amount of growth factor used in the earlier simulations. Since we are interested only in a general assessment of autocrine effects, we did not vary the secretion rate based on cell maturity.

In the proliferation-driven system, autocrine growth factor production made the steady state unstable; simulations with cell counts below the steady-state point died out, while those with cell counts above the steady-state grew without bound. In contrast, simulations with monocyte influx were still stable, but the final cell counts were slightly lower in the high-efflux runs.

In the paracrine system, cells reduced ligand concentration through consumption. In the autocrine system, the net effect is to increase ligand concentration. The negative feedback described in section 4.3 has been changed to a positive feedback. In the proliferation-driven system, this works to drive the system away from the ligand concentration at which $k = l$. However, the influx-driven system is stable even without this negative feedback; autocrine rather than paracrine production may change the location of the steady state, but not its stability.

8 Related Work

There are numerous models of cell division which do not depend on extracellular signals, although the idea of dividing the cell cycle into variable- and fixed-length periods has been around for some time. Smith and Martin (1973) proposed that the switch from the variable-length 'A-state' to the fixed-length 'B-state'—apparently comparable to the restriction point notion mentioned in section 4—is random. Many more recent models ((e.g., Tyrcha, 2001)) treat the probability as dependent on cell age or cell mass; Tyrcha points out that 'mass' may represent cumulative mitogen signalling. In other cases, there is no distinction between the different parts of the cell cycle, but the population growth rate depends on the growth factor concentration (Lauffenburger and Linderman, 1993). These models represent cells growing in high concentrations of growth factor, so ligand depletion is often ignored.

A model described in Morel *et al.* (1996) and Burke *et al.* (1997) of T cell growth in response to IL-2 and IL-4 has some similarities to our models. They use a distribution of receptor synthesis values to capture heterogeneity in the cellular responses to ligand. They also divide the cell cycle into variable and fixed portions, where the former depends on cells accumulating a certain number of binding events. However, their focus is on synergy between two

growth factors in conditions of fairly high growth factor concentration, and they do not include cell death.

SIMMUNE is another multi-purpose simulator for individual cell interactions and responses to molecular signals. Meier-Schellersheim (2001) developed it to study intercellular interactions in the immune system. SIMMUNE connects discrete behaviors of individual cells to receptor-mediated interactions with other cells and the (continuous) molecular environment.

9 Discussion

In this paper, we used both mathematical modeling and simulation to explore growth factor regulation of macrophage populations and its effect on peripheral effector homeostasis. Our modeling suggests that certain experimental measurements would help clarify macrophage behavior. More detailed information on death rates in normal cell cultures or the kinetics of death in individual cells would help refine the basic model of cell behavior. The homeostasis model predicts a correlation between monocyte influx and higher macrophage loss rates; it might be possible to confirm this correlation either directly or by testing for expression of adhesion molecules involved in monocyte trafficking.

Our model includes growth factor regulation of both cell proliferation and cell survival. The proliferative response takes into account the time required both for a cell to prepare to divide and for completion of the cell cycle. We use a very simple scheme for the effect of growth factor on a cell's progression towards the restriction point; it may become necessary in the future to more explicitly represent the interaction between positive and negative regulation of cell responses to cytokine signals rather than just considering the net effect. By contrast with the proliferative response, we assume cell death is essentially a random process, although a cell's probability of dying depends on the growth factor concentration. This model gave good agreement with available culture data relating macrophage population size to growth factor concentration. However, the simulation death rates seemed to be uncharacteristically high under some circumstances, which may indicate that we have oversimplified the role of cell state in the death process.

We studied two alternative hypotheses regarding maintenance of the alveolar macrophage pool: one in which cells are replenished solely through local proliferation, and one in which migration from circulation is a primary source of new cells. We found that proliferation-driven homeostasis should be associated with lower cell loss rates, while influx-driven homeostasis is associated with higher loss rates. It is very likely that both mechanisms are used, but each might dominate under different circumstances.

In our model, cell consumption of growth factor was significant, and the resulting negative feedback was essential for stability of the population replenished only through local proliferation. Whether or not ligand depletion is relevant for a particular molecular mediator depends on the binding properties of that ligand and its receptor, but we cannot always assume that cellular responses depend simply on the molecular concentration; the cell density may also affect the signal each cell actually sees. Autocrine regulation is another mechanism for which the effects depend on the context of the entire system. We found that purely autocrine regulation is potentially destabilizing but can work in combination with other regulatory mechanisms.

Connecting extracellular signals to individual cell actions is difficult because intracellular signalling is very complex and incompletely understood. Many of the individual processes involved between receptor-ligand binding and the final observable event occur on different timescales and stochastic effects may be important. Our approach abstracts much of the intracellular signalling complexity, while capturing the aspects most likely to affect intercellular dynamics.

We expect spatial effects to be important in many multicellular models. For the homeostasis models presented here, the primary source of spatial heterogeneity would be the number and location of cells secreting growth factor. In the autocrine system, or a paracrine system in which many cells contribute to the growth factor concentration, the results of spatially explicit simulations are similar to those presented here for homogeneous molecular concentration. Results are significantly different if growth factor is supplied by a small number of sparsely distributed tissue cells, in which case the rate of molecular diffusion and manner of cell movement are also important. However, very little is currently known about actual secretion rates or spatial distribution of cytokines and macrophages *in vivo*, so we leave the important issue of spatial effects for future work.

Our simulator introduces a general framework for cell responses to molecular signals that can be applied to other models. As more data become available on individual cell characteristics, we will be able to relate those observations to intercellular interactions. This sort of approach will be useful in studying the dynamics of localized tissue microenvironments. We plan to use our models of homeostatic regulation as a baseline for future studies of more complex regulatory networks; we are particularly interested in granuloma formation in tuberculosis (Warrender *et al.*, 2003). Models such as those presented here can improve our understanding of the relative importance of different kinds of regulation in immunological systems.

10 Acknowledgments

The authors gratefully acknowledge the partial support of the National Institutes of Health (P20 GM066283), the National Science Foundation (grants ANIR-9986555, CCR-0311686, and DBI-0309147), Defense Advanced Research Projects Agency (grants AGR F30602-00-2-0584 and F30602-02-1-0146), the Intel Corporation, and the Santa Fe Institute. Dennis Chao and an anonymous referee provided many helpful suggestions.

References

Akagawa, K. S., K. Kamoshita, and T. Tokunaga (1988). Effects of granulocyte-macrophage colony-stimulating factor and colony-stimulating factor-1 on the proliferation and differentiation of murine alveolar macrophages. *Journal of Immunology* **141**(10), 3383–3390.

Becker, S., R. B. Devlin, and J. S. Haskill (1989). Differentiatial production of tumor necrosis factor, macrophage colony stimulating factor, and interleukin 1 by human alveolar macrophages. *Journal of Leukocyte Biology* **45**(4), 353–361.

Blusse van Oud Alblas, A., H. Mattie, and van R. Furth (1983). A quantitative evaluation of pulmonary macrophage kinetics. *Cell and Tissue Kinetics* **16**(3), 211–9.

Blusse van Oud Alblas, A. and R. van Furth (1979). Origin, kinetics and characteristics of pulmonary macrophages in the normal steady state. *Journal of Experimental Medicine* **149**, 1504–1518.

Bowden, D. H. (1984). The alveolar macrophage. *Environmental Health Perspectives* **55**, 327–341.

Burke, M. A., B. F. Morel, T. B. Oriss, J. Bray, S. A. McCarthy, and P. A. Morel (1997). Modeling the proliferative response of T cells to IL-2 and IL-4. *Cellular Immunology* **178**(1), 42–52.

Chen, B. D., C. K. 3rd, and H. S. Lin (1984). Receptor-mediated binding and internalization of colony-stimulating factor (csf-1) by mouse peritoneal exudate macrophages. *Journal of Cell Science* **70**, 147–66.

Chen, B. D., T. Chou, and C. R. Clark (1987). Delineation of receptor-mediated colony-stimulating factor (CSF-1) utilization and cell production by precursors of mononuclear phagocytic series at various stages of differentiation. *British Journal of Haematology* **67**(4), 381–386.

Chen, B. D., M. Mueller, and T. H. Chou (1988). Role of granulocyte/macrophage colony-stimulating factor in the regulation of murine alveolar macrophage proliferation and differentiation. *Journal of Immunology* **141**(1), 139–144.

Coggle, J. E. and J. D. Tarling (1984). The proliferation kinetics of pulmonary alveolar macrophages. *Journal of Leukocyte Biology* **35**(3), 317–327.

Corry, D., P. Kulkarni, and M. F. Lipscomb (1984). The migration of bronchoalveolar macrophages into hilar lymph nodes. *American Journal of Pathology* **115**(3), 321–328.

Fisher, E. S., D. A. Lauffenburger, and R. P. Daniele (1988). The effect of alveolar macrophage chemotaxis on bacterial clearance from the lung surface. *American Review of Respiratory Disease* **137**, 1129–1134.

Fritsch, P. and R. Masse (1992). Overview of pulmonary alveolar macrophage renewal in normal rats and during different pathological processes. *Environmental Health Perspectives* **97**, 59–67.

Guilbert, L. J. and E. R. Stanley (1986). The interaction of 125i-colony-stimulating factor-1 with bone marrow-derived macrophages. *The Journal of Biological Chemistry* **261**(9), 4024–32.

Harmsen, A. G., B. A. Muggenburg, M. B. Snipes, and D. E. Bice (1985). The role of macrophages in particle translocation from lungs to lymph nodes. *Science* **230**, 1277–1280.

Held, T. K., M. E. A. Mielke, M. Unger, M. Trautmann, and A. S. Cross (1996). Kinetics and dose dependence of macrophage colony-stimulating factor-induced proliferation and activation of murine mononuclear phagocytes in situ: Differences between lungs, liver and spleen. *Journal of Interferon and Cytokine Research* **16**, 159–168.

Lanza, R. P., R. Langer, and J. Vacanti, eds. (2000). *Principles of Tissue Engineering*. Academic Press.

Laskin, D. L., B. Weinberger, and J. D. Laskin (2001). Functional heterogeneity in liver and lung macrophages. *Journal of Leukocyte Biology* **70**(2), 163–70.

Lauffenburger, D. A. and J. J. Linderman (1993). *Receptors: Models for binding, trafficking, and signaling*. Oxford University Press.

Lin, H., B. L. Lokeshwar, and S. Hsu (1989). Both granulocyte-macrophage CSF and macrophage CSF control the proliferation and survival of the same subset of alveolar macrophages. *The Journal of Immunology* **142**(2), 515–519.

Meier-Schellersheim, M. (2001). *The immune system as a complex system: Description and simulation of the interactions of its constitutents*. Ph.D. thesis, University of Hamburg, Hamburg, Germany.

Metcalf, D. (1991). Control of granulocytes and macrophages: molecular, cellular, and clincial aspects. *Science* **254**(5031), 529–533.

Morel, B. F., M. A. Burke, J. Kalagnanam, S. A. McCarthy, D. J. Tweardy, and P. A. Morel (1996). Making sense of the combined effect of interleukin-2 and interleukin-4 on lymphocytes using a mathematical model. *Bulletin of Mathematical Biology* **58**(3), 569–594.

Pardee, A. B. (1989). G1 events and regulation of cell proliferation. *Science* **246**(4930), 603–608.

Perez-Arellano, J. L., M. C. Alcazar-Montero, and A. Jimenez-Lopez (1990).

Alveolar macrophage: origin, kinetics and relationship with cells of the alveolo-interstitial region. *Allergologia et immunopathologia (International Journal for clinical and investigative allergology and clinical immunology)* **18**(3), 175–183.

Shellito, J., C. Esparza, and C. Armstrong (1987). Maintenance of the normal rat alveolar macrophage cell population. *American Review of Respiratory Disease* **135**(1), 78–82.

Smith, J. A. and L. Martin (1973). Do cells cycle? *Proceedings of the National Academy of Sciences U S A* **70**(4), 1263–7.

Smith, K. A. (1989). The interleukin 2 receptor. *Annual Review of Cell Biology* **5**, 397–342.

Stanley, E. R. and D. Metcalf (1971). Enzyme treatment of colony stimulating factor: evidence for a peptide component. *The Australian Journal of Experimental Biology and Medical Science* **49**(3), 281–90.

Tushinski, R. J., I. T. Oliver, L. J. Guilbert, P. W. Tynan, J. R. Warner, and E. R. Stanley (1982). Survival of mononuclear phagocytes depends on a lineage-specific growth factor that the differentiated cells selectively destroy. *Cell* **28**, 71–81.

Tushinski, R. J. and E. R. Stanley (1985). The regulation of mononuclear phagocyte entry into S phase by the colony stimulating factor CSF-1. *Journal of Cellular Physiology* **122**, 221–228.

Tyrcha, J. (2001). Age-dependent cell cycle models. *Journal of Theoretical Biology* **213**(1), 89–101.

van Furth, R. (1992). Production and migration of monocytes and kinetics of macrophages. In R. van Furth, ed., *Mononuclear Phagocytes*, pp. 3–12. Kluwer Academic Publishers.

Warrender, C., S. Forrest, and L. Segel (2003). Modeling intercellular signalling in tuberculosis. In *4th International Conference on Systems Biology*, pp. 268–269. St. Louis, Missouri.

Williams, G. T., C. A. Smith, E. Spooncer, T. M. Dexter, and D. R. Taylor (1990). Haemopoietic colony stimulating factors promote cell survival by suppressing apoptosis. *Nature* **343**(6253), 76–79.

Zandstra, P. W., D. A. Lauffenburger, and C. J. Eaves (2000). A ligand-receptor signaling threshold model of stem cell differentiation control: a biologically conserved mechanism applicable to hematopoiesis. *Blood* **96**(4), 1215–22.